# Emission Performance of Low Cetane Naphtha as Drop-In Fuel on a Multi-Cylinder Heavy-Duty Diesel Engine and Aftertreatment System

**Author, co-author (Do NOT enter this information. It will be pulled from participant tab in MyTechZone)**

Affiliation (Do NOT enter this information. It will be pulled from participant tab in MyTechZone)

## Abstract

Greenhouse gas regulations and global economic growth are expected to drive a future demand shift towards diesel fuel in the transportation sector. This may create a market opportunity for cost-effective fuels in the light distillate range if they can be burned as efficiently and cleanly as diesel fuel. In this study, the emission performance of a low cetane number, low research octane number naphtha (CN 34, RON 56) was examined on a production 6-cylinder heavy-duty on-highway truck engine and aftertreatment system. Using only production hardware, both the engine-out and tailpipe emissions were examined during the heavy-duty emission testing cycles using naphtha and ultra-low-sulfur diesel (ULSD) fuels. Without any modifications to the hardware and software, the tailpipe emissions were comparable when using either naphtha or ULSD on the heavy duty test cycles. Overall lower $CO_2$ emissions and fuel consumption were measured for naphtha due in part to its higher heating value and higher hydrogen to carbon ratio. Engine-out and tailpipe NOx emissions were lower for naphtha, and measured PM emissions were also lower due to naphtha's higher volatility and lower aromatic content compared to ULSD. To help assess the potential impact on diesel particulate filter design and operation, engine-out PM samples were collected and characterized at a steady-state mid-speed, mid-load operating point. A significant reduction in elemental carbon in PM samples was observed for naphtha fuel, and similar oxidation rates and peak oxidation temperatures were measured for the PM from both fuels.

## Introduction

Diesel engines offer high fuel efficiency, good driving performance, and reduced carbon dioxide emissions compared to stoichiometric gasoline or natural gas engines. Commercial vehicle applications also tend to require high energy density, so the potential for electrification is somewhat limited compared to passenger car applications. For these reasons, diesel engines are expected to remain the prime workhorse for commercial transportation into the foreseeable future. This will lead to substantial demand for middle distillate fuels at the same time that demand for fuels in the gasoline range is expected to weaken [1-3]. Such a demand imbalance will present market opportunities for light distillate fuels that can be burned as efficiently as diesel fuel.

Conventional diesel combustion is intrinsically stratified and mixing-controlled, and offers good controllability at the expense of high NOx and soot emissions. Naphtha, which has a low cetane number (CN) and low research octane number (RON), has been tested for mixing controlled combustion [4-6]. As one of the refinery streams with a similar boiling point range as gasoline, these fuels can be easily produced, and could help reduce well-to-wheel $CO_2$ emissions. In a previous study, significant reductions in soot and NOx emissions with similar fuel efficiency were obtained with naphtha fuel in an on-highway heavy-duty diesel engine [4]. Moreover, experimental results showed that when engine compression ratio is sufficiently high, the resulting cylinder pressure and temperature are adequate to suppress the reactivity difference between lighter end fuels and diesel at medium-to-high engine load. Consequently, naphtha and diesel exhibited similar global combustion behavior at the conditions closely representative of on-highway vehicle operation. Based on these experimental observations, naphtha fuel could potentially be used as a replacement for diesel fuels under mixing-controlled combustion for heavy-duty truck engine applications [4].

Diesel engine exhaust contains different phases of pollutants, and requires a complex aftertreatment system. In addition to gaseous pollutants like carbon monoxide (CO) and hydrocarbons (HC), particulate matter (PM) consists of dry carbon (soot) and soluble organic fraction (SOF), which includes liquid-phase unburned and partially decomposed fuel and lubricant oil. As it is difficult to reduce nitrogen oxides ($NOx = NO + NO_2$) under lean exhaust conditions, various lean NOx reduction catalyst technologies have been developed. Currently, selective catalytic reduction (SCR) technology, which reduces NOx with ammonia ($NH_3$) as the reductant, is most widely used due to its excellent NOx reduction efficiency over a wide range of temperatures, and lower overall system cost.

A typical aftertreatment system using SCR technology consists of a diesel oxidation catalyst (DOC), a catalyzed diesel particulate filter (DPF), SCR catalyst, and ammonia slip catalyst (ASC), which are placed in a specific order to achieve a desired level of emission reduction performance. First, engine-out emissions are reduced by exhaust gas recirculation (EGR), which is often cooled to further reduce the peak combustion temperature. HC, CO, and NO are oxidized by a DOC, and PM is trapped and oxidized over a DPF. Aqueous urea solution, which is marketed as diesel exhaust fluid (DEF) in the USA, is injected into the hot exhaust, and decomposes to $NH_3$. NOx is then reduced by $NH_3$ over an SCR catalyst, and excess $NH_3$ is removed by an ASC.

Although particulate matter (PM) is easily trapped by a filter, trapped PM must be oxidized to $CO_2$ in order for the DPF to remain effective. Particulate matter can be oxidized during normal operation through $NO_2$-assisted "passive soot oxidation" or by $O_2$ during periodic high-temperature "active filter regeneration" events. As a result, diesel aftertreatment systems are typically designed and operated around the DPF regeneration strategy. For example, more durable DOC and SCR catalyst formulations must be used when more frequent active filter regenerations are expected during the lifetime of the system. Therefore, it is important to understand the effects of fuels on the chemistry and kinetics of soot oxidation.

As a first step to introduce light distillate fuels for heavy-duty diesel engine applications, it is important to evaluate the performance and compatibility with existing engine-aftertreatment systems. Therefore, in this study, a low CN, low RON naphtha fuel (CN 34, RON 56) was evaluated as a drop-in fuel replacement using the current production MY2013 ISX15 heavy-duty diesel engine and aftertreatment system. The effects of fuels on both the engine-out and tailpipe emissions were compared against ultra-low-sulfur diesel (ULSD) fuel during the EPA heavy-duty transient test cycle. The effects of fuels on engine performance and emissions were further compared at the steady-state B50 operating point (i.e., 50% load at B speed on the engine map). In addition, engine-out PM samples were analyzed to assess the fuels' effects on the chemical composition in terms of elemental carbon (EC) and organic carbon (OC), and the oxidation rates.

## Experimental Setup

### *Engine and Instrumentation*

All the experiments were performed with a MY2013 Cummins ISX15 engine and aftertreatment system. This engine is equipped with a common rail injection system capable of 2500 bar fuel injection pressure, a single-stage variable geometry turbocharger (VGT), a cooled high pressure EGR loop, and a charge air cooler (CAC). The aftertreatment system includes a DOC, a catalyzed DPF, an SCR and an ASC in a straight, single leg configuration. The DEF supply system, which consists of a storage tank and a pump, is connected to a DEF doser that is installed on the decomposition tube, where urea decomposes to $NH_3$ in the hot exhaust gas. Both the engine and aftertreatment system were controlled by Cummins' proprietary software and calibrations. The engine and aftertreatment specifications are summarized in Table 1.

Table 1. Engine and aftertreatment system specifications

| | |
|---|---|
| Engine Type | 4-valve Compression Ignition |
| Displacement Volume | 14.9 L |
| Number of Cylinders | 6 |
| Bore | 137 mm |
| Stroke | 169 mm |
| Compression Ratio | 18.9 |
| Diesel Fuel System | 2500 bar common rail |
| Air System | Single-stage VGT<br>High pressure EGR loop with cooling<br>Charge air cooler |
| Engine Ratings | 236 kW @ 1800 rpm<br>2375 N-m @ 1000 rpm |
| Aftertreatment System | Straight, single-leg configuration<br>DOC/DPF, SCR/ASC modules<br>Temperature, pressure, NOx, $NH_3$ sensors |

All engine testing was conducted on an AC engine dynamometer at Aramco Research Center – Detroit. The cooling system and air system restrictions were set to the manufacturer recommendations. Crank angle (CA) resolved cylinder pressure measurements were acquired using Kistler 6067C water-cooled pressure transducers in all six cylinders. High speed data acquisition and processing was conducted using AVL IndiModul hardware together with the Indicom software package. Fuel flow was measured using the AVL FuelExact Coriolis mass flow measurement unit, while intake air flow rate was measured using the AVL Flowsonix Air unit based on an ultrasonic transit time difference method. Extra cooling of the fuel return line was implemented to prevent boiling of the naphtha fuels. Before testing, the factory new aftertreatment system was degreened for 15 hours at rated power.

### *Fuels*

Fuels tested in this study are a US market ULSD fuel, and a low CN, low RON naphtha fuel. This naphtha fuel was derived directly from crude oil during the distillation process, but was doped with Infineum R650 lubricity additive at 200 ppm to alleviate any potential problems with the fuel injection system. This level of additive was determined through wear scar testing, which compared the wear scar patterns of naphtha fuels against that of ULSD fuel (ASTM D6079). The analysis of the fuels' chemical compositions was also performed by using the Fluorescent Indicator Adsorption (FIA) method (ASTM D1319). Some of the major properties of the two fuels are listed in Table 2.

Table 2. Fuel properties of tested fuels

| Fuel | ULSD | Naphtha |
|---|---|---|
| Research Octane Number | - | 56.0 |
| Motor Octane Number | - | 55.1 |
| Cetane Number | 41.2 | 34.1 |
| Specific Gravity at 15.56 ºC [g/mL] | 0.854 | 0.715 |
| Gross Heating Value [MJ/kg] | 45.557 | 47.261 |
| Net Heating Value [MJ/kg] | 42.760 | 44.112 |
| Kinematic Viscosity [$mm^2$/sec] | 2.42 | 0.59 |
| Saturates [vol%] | 69.5 | 91.7 |
| Olefins [vol%] | 1.5 | 0.4 |
| Aromatics [vol%] | 29.0 | 8.0 |
| Sulfur [ppm] | 5.9 | 10.9 |
| H/C ratio [mol/mol] | 1.82 | 1.86 |

### *Test Conditions*

In this study, both heavy-duty transient and steady-state tests were conducted following the EPA regulatory procedures, and the test results were analyzed using AVL's iGEM and Concerto software. The heavy-duty FTP test cycle simulates light urban traffic, crowded urban traffic, and crowded expressway traffic conditions. Typically,

this test cycle is repeated twice (one cold start and a subsequent hot start with a 1200-second soak in between), and the combined emissions results are reported for certification purposes. During this study, one cold FTP (cFTP) and three hot FTP (hFTP) tests were performed for each fuel. The ramped modal cycle (RMC) tests, which are required by EPA for emission certifications, were also performed for both fuels. All the tests were conducted without any modifications to the engine calibration, although a separate torque map was generated for each fuel. There were no challenges associated with following the transient speed and torque command, and all the test results passed the statistical tests for cycle validation with both fuels.

In addition to transient emissions testing, steady-state emissions testing was performed at the B50 operating point, which describes a mid-speed (B speed) mid-load (50% torque) point on the engine map (i.e., 1375 rpm, 10 bar IMEP for this engine), to assess the effects of fuels on combustion and emissions, and to collect engine-out PM samples for analysis. For this testing, constant NOx emissions and CA50, which is defined as the crank angle position where 50% of the heat is released, were maintained by adjusting the EGR rate and fuel injection timing. Fuel injection pressure was fixed at 1450 bar.

### *Emissions Sampling*

Exhaust emissions were examined from the engine-out to tailpipe locations across the aftertreatment system. Exhaust emissions were measured using a Horiba Mexa-7500D emissions bench. A standard heated chemiluminescence detector (CLD) and a flame ionization detector (FID) were used for measuring $NO_x$ and HC emissions, respectively. The CO and intake/exhaust $CO_2$ emissions were measured using non-dispersive infrared (NDIR) instruments. A paramagnetic detector (PMD) was used to measure the exhaust $O_2$ concentration. Both a smoke meter (AVL 415SE) and a micro soot sensor (AVL 483 MSS) were used to collect engine-out PM information in the form of filtered smoke number (FSN) and soot concentration ($mg/m^3$), respectively. In addition, an AVL SESAM i60 Fourier Transform infrared spectrometer (FTIR) unit with an optical path length of 5.11 m and a liquid-$N_2$ cooled Mercury Cadmium Telluride (MCT) detector was used to monitor tailpipe $NH_3$ and $N_2O$ emissions. The gas cell was operated at a pressure of 800 mbar and a temperature of 191 °C. Measurement scans were performed at 1 Hz with a spectral resolution of 0.5 $cm^{-1}$.

### *Particulate Matter Sampling and Analysis*

Engine-out PM samples were taken using both raw exhaust sampling and single-stage dilution, as shown in Figure 1. Raw exhaust PM sampling was used to collect enough PM material for thermogravimetric analysis (TGA), and the single-stage dilution sampling was used to collect PM for mass quantification and chemical analysis. A beveled probe was placed downstream of the turbocharger with a 45º cut facing the engine-out exhaust. Heated lines were used to maintain the exhaust flow temperature at 190ºC. The sampling manifold had three splits, sending exhaust flow to two separate heated filter ovens and a single-stage dilution tunnel. At 50ºC, both ovens maintained the raw exhaust gas temperature at 5ºC above the dew point to minimize the volatilization of organics from the PM and prevent the condensation of water vapor onto the PM sample. The TGA samples were collected on pre-fired, 47-mm diameter, quartz-fiber filters (QFF) located in one of the heated ovens. Water vapor was condensed after the QFF by two impingers in an ice water bath prior to the pump and dry gas meter.

Samples for TGA were cut from the QFF using a 9-mm diameter arch punch which was the maximum diameter sample size that could fit into the TGA weighing pans. Two 9-mm disks from the same filter were measured together in each TGA analysis, and three separate TGA analysis runs were performed for each fuel sample. Data recorded for each fuel are averages from the three TGA analysis runs. TGA was performed using a TA Instruments Q5000 IR TGA with a Pfeiffer Omnistar mass spectrometer (MS). Samples were first held at 50 °C for 30 minutes in $N_2$ and were then heated in dry air at 5°C/min to 800°C and held for 30 minutes.

Flow sent to the dilution tunnel was maintained at 190ºC and controlled by a critical orifice and ejector pump which was diluted with dry, filtered air using a mass flow controller. The diluted exhaust was maintained at 45ºC for PM sampling. A primary QFF was collected for elemental carbon (EC) and organic carbon (OC) analysis. In parallel, a second set of filter samples was collected in series, first through a Teflon membrane filter (TF, Pall Teflo) followed by secondary QFF. The TF filters were weighed before and after sampling for PM mass measurement. The secondary QFF was also analyzed for EC-OC content using the NIOSH method [7]. The measured organics absorbed on the secondary QFF were subtracted from the primary QFF OC content to correct for filter adsorption artifacts [8,9].

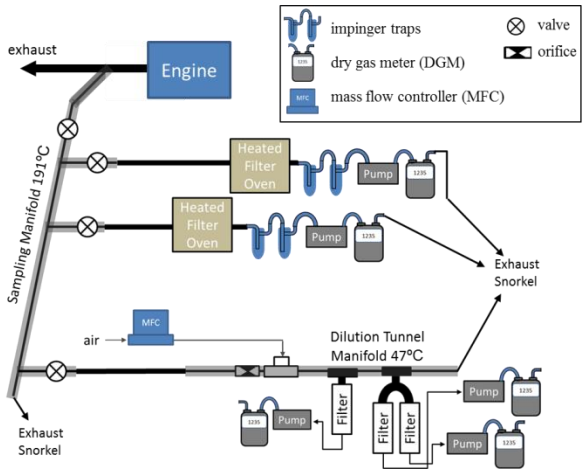


Figure 1. The basic layout of the PM filter sampling set-up is shown. The sampling manifold line was inserted into the center of the engine exhaust pipe with a 45º beveled edge facing the exhaust flow. Heated sample lines (thick black lines) and heat tape (grey overlay lines) were used to maintain the temperature in the manifolds. Heated filter ovens were maintained above the dew point at 50 ºC Additional by pass lines and valves used are omitted for clarity.

## Results and Discussion

### *Fuel Effects on Engine-Out Emissions during Transient Testing*

The effects of naphtha and ULSD fuels on engine-out (EO) emissions during transient emission testing are summarized in Table 3 and Table 4. As shown in Table 3, lower engine-out $CO_2$ and lower fuel consumption (FC) were observed for naphtha fuel compared to ULSD fuel. Fuel injection calibration, such as injection timing and pulse width, was kept the same for both fuels. Since the volumetric

fuel injection was fixed for the two fuels, and the naphtha fuel has a lower density, less mass of the naphtha was injected compared to ULSD. However, the work was practically equivalent despite this injected mass difference for the two fuels. Thus, the observed difference in fuel consumption was attributed to the higher heating value and H/C ratio for the naphtha fuel.

Table 3. Fuel effects on engine-out gaseous emissions, fuel consumption and work done during the tests

| EO Emissions | | $CO_2$ | CO | THC | FC | Work |
|---|---|---|---|---|---|---|
| | | g/kWh | g/kWh | g/kWh | g/kWh | kW |
| ULSD | cFTP | 774 | 0.81 | 0.84 | 244 | 23.2 |
| | hFTP | 725 | 0.70 | 0.75 | 228 | 23.3 |
| | RMC | 612 | 0.31 | 0.11 | 192 | 118.0 |
| Naphtha | cFTP | 711 | 1.61 | 0.95 | 230 | 23.4 |
| | hFTP | 683 | 1.48 | 0.57 | 221 | 23.4 |
| | RMC | 588 | 0.48 | 0.12 | 189 | 118.3 |

Engine-out NOx and soot emissions based on the MSS were generally, slightly lower for naphtha fuel during the FTP and RMC testing (shown in Table 4). In our previous study, we have shown that the naphtha fuel can help improve the fuel-air mixing for PPCI combustion at a lower compression ratio (CR) of 17 [2]. This slight yet consistent reduction in emissions suggests that the higher volatility and lower reactivity of naphtha fuel can still help improve the fuel-air mixing before the start of combustion even at a relatively high CR of 19. Overall NOx/PM ratio was about the same for both fuels, which suggests that soot loading and unloading behavior would be similar during normal DPF operation.

Table 4. Fuel effects on engine-out NOx and PM emissions during transient tests

| EO Emissions | | NOx | MSS | NOx/PM |
|---|---|---|---|---|
| | | g/kWh | mg/kWh | |
| ULSD | cFTP | 4.23 | 124 | 34 |
| | hFTP | 4.93 | 70 | 70 |
| | RMC | 4.88 | 19 | 256 |
| Naphtha | cFTP | 4.37 | 117 | 37 |
| | hFTP | 4.21 | 70 | 60 |
| | RMC | 4.34 | 17 | 257 |

## *Fuel Effects on Tailpipe Emissions*

The effects of fuels on tailpipe (TP) emissions are summarized in Table 5. Engine-out CO and gaseous HC were easily oxidized to $CO_2$ over the DOC and DPF catalyst for both fuels. Lower tailpipe $CO_2$ was obtained with naphtha fuel, confirming its lower fuel consumption compared to ULSD fuel. Tailpipe NOx was slightly higher for both the naphtha and ULSD fuels during the cold FTP test, but lower during the hot FTP and RMC tests.

Table 5. Fuel effects on tailpipe NOx and PM emissions

| TP Emissions | | $CO_2$ | CO | THC | NOx |
|---|---|---|---|---|---|
| ULSD | cFTP | 772 | 0.02 | 0.03 | 0.71 |
| | hFTP | 728 | 0.00 | 0.01 | 0.25 |
| | RMC | 618 | 0.03 | 0.00 | 0.20 |
| Naphtha | cFTP | 712 | 0.34 | 0.12 | 0.74 |
| | hFTP | 675 | 0.09 | 0.04 | 0.19 |
| | RMC | 592 | 0.03 | 0.00 | 0.18 |

*All values reported in g/kW-hr

On-highway heavy-duty diesel engines in the USA need to meet the 0.20 g/hp-hr NOx emission standard over heavy-duty transient cycle testing. SCR NOx reduction performance is dependent on numerous parameters, such as catalyst formulation, exhaust gas flow rate, temperature, catalyst size, substrate cell density, DEF dosing rate, and stored $NH_3$ amount. In this study, the SCR system was operated by Cummins' proprietary controls, which consistently achieved a high level of NOx reduction for both fuels. As shown in Table 6, the same level of NOx reduction performance was obtained for both fuels. The weighted FTP and RMC results for the naphtha fuel were below the 0.2 g/hp-hr threshold.

Table 6. Fuel effects on engine-out and tailpipe NOx and PM emissions

| NOx Reduction | | EO NOx | TP NOx | %NOx |
|---|---|---|---|---|
| | | g/hp-hr | g/hp-hr | |
| ULSD | cFTP | 3.16 | 0.53 | 83 |
| | hFTP | 3.68 | 0.19 | 95 |
| | RMC | 3.64 | 0.15 | 96 |
| Naphtha | cFTP | 3.26 | 0.55 | 83 |
| | hFTP | 3.14 | 0.14 | 96 |
| | RMC | 3.24 | 0.13 | 96 |

In addition, Table 7 compares the tailpipe $NH_3$ and $N_2O$ emissions for the two fuels. Currently, $NH_3$ emissions are not regulated by EPA, but it is considered important for ambient air quality and customer comfort. As urea decomposes into $NH_3$ before reacting with NOx over an SCR catalyst, high tailpipe $NH_3$ emission can occur when excess $NH_3$ stored on the SCR catalyst desorbs during the third phase of the FTP test. However, because an ammonia slip catalyst (ASC) is used downstream of the SCR catalyst in the current system configuration, there was no $NH_3$ breakthrough during any of the tests, as shown in Table 7.

Unlike the criteria pollutants, $N_2O$ is regulated as part of greenhouse gas (GHG) regulations at 0.1 g/hp-hr, because of its high global warming potential. Formation of $N_2O$ over the diesel aftertreatment system can be traced to multiple sources, including NOx reduction by hydrocarbons over the DOC and decomposition of ammonium nitrate over the SCR catalyst. As shown in Table 7, similarly low levels of tailpipe $N_2O$ emissions were reported for both fuels.

Table 7. Fuel effects on tailpipe $NH_3$ and $N_2O$ emissions

| TP Emissions | | $NH_3$ | $N_2O$ |
|---|---|---|---|
| | | g/hp-hr | g/hp-hr |
| ULSD | cFTP | 0.00 | 0.07 |
| | hFTP | 0.00 | 0.08 |
| | RMC | 0.00 | 0.08 |
| Naphtha | cFTP | 0.00 | 0.10 |
| | hFTP | 0.00 | 0.09 |
| | RMC | 0.00 | 0.06 |

## *Fuel Effects on Engine Performance and Emissions at B50*

To further understand the impact of naphtha on engine combustion and emissions behavior, steady-state engine testing was conducted at the B50 operating point, which is a mid-speed, mid-load point on the engine map (i.e., 1375 rpm, 10 bar IMEP for this engine), for ULSD and naphtha fuels. Engine-out NOx emissions were maintained at 4.7 g/kw-hr for both fuels by adjusting the EGR rate. The CA50 was also maintained at the same 6˚ATDC, while fuel injection pressure was fixed at 1450 bar.

As shown in Figure 2, a significant reduction in filter smoke number (FSN) was achieved with naphtha fuel at an equivalent level of engine-out NOx emissions. In addition, approximately 3% reduction in brake specific fuel consumption (BSFC) was observed for naphtha fuel. This difference could be largely attributed to the different lower heating values between the two fuels (shown in Table 2), and is further supported by the same level of engine brake thermal efficiency (BTE) observed for both fuels. It is also worth noting that both naphtha and ULSD fuels exhibited similar ignition delay times, suggesting that the cylinder pressure and temperature at B50 may be sufficiently high enough to suppress any effects of fuel reactivity differences on engine performance.

A more pronounced premixed combustion peak was also observed for naphtha fuel (as shown in Figure 3). Considering the similar ignition delay times, the higher volatility and lower viscosity of the naphtha fuel might explain this combustion behavior and contribute to the lower soot emissions compared to ULSD fuel. As the overall combustion was still dominated by mixing-controlled combustion, the lower naphtha-fuel soot emissions might also be attributed to its lower aromatic content [10].

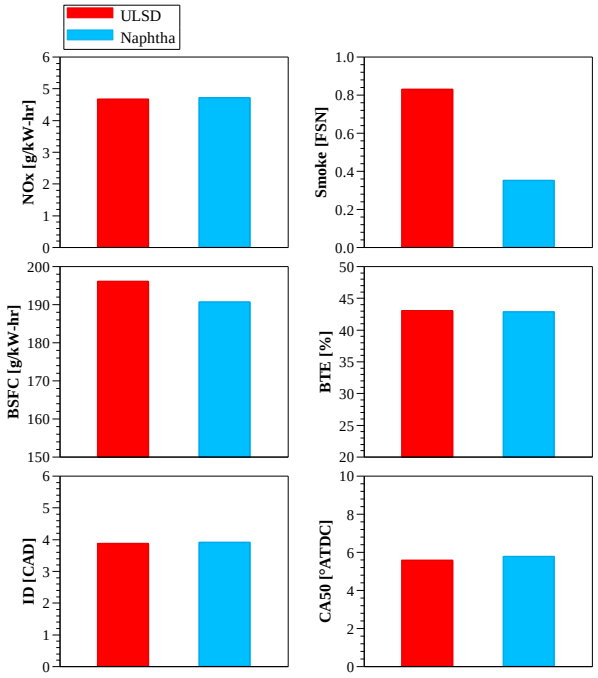


Figure 2. Engine performance and emissions for ULSD and naphtha fuels at B50

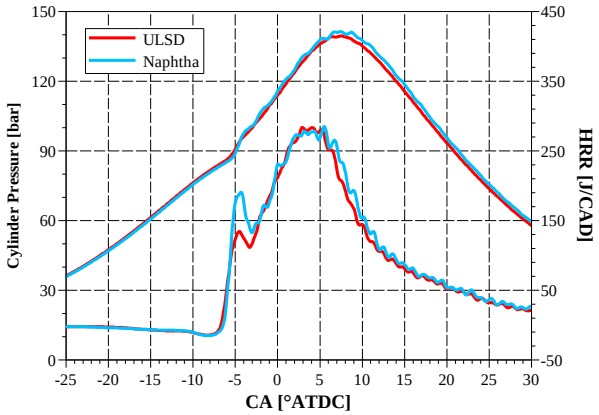


Figure 3. Cylinder pressure (upper curves) and heat release rate (lower curves) at B50

## *Fuel Effects on Particulate Matter Chemistry*

Engine-out PM samples at the B50 operating point were further analyzed to assess the fuels' effects on their chemical composition and oxidation rates. Figure 4 shows the total carbon (TC) as measured on the Teflon filters (TF), and the PM chemical compositions in terms of elemental carbon (EC) and organic carbon (OC) as measured following the NIOSH method [16]. Figure 4 indicates that USLD produces twice as much TC as does naphtha (15.0 mg/m$^3$ and 7.6 mg/m$^3$, respectively), and is consistent with the lower FSN from naphtha fuel (as shown in Figure 2). While slightly more OC was present in the ULSD PM (3.9 mg/m$^3$) than the naphtha PM (2.9 mg/m$^3$), the OC accounted for a larger fraction of the total naphtha PM, 36%, compared to only 26% for ULSD. The significant reduction in total PM with the naphtha fuel can therefore be primarily

attributed to its reduced EC content (i.e. 4.2 mg/m$^3$) compared to ULSD PM (10.8 mg/m$^3$). Since OC can be easily oxidized over DOC and DPF catalysts, this finding suggests that it may be possible to further reduce high-temperature active filter regeneration frequency with naphtha fuel, thus improving the fuel economy and aftertreatment system durability.

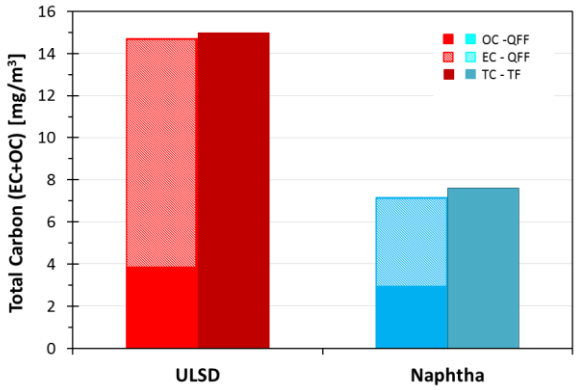


Figure 4. Filter mass measurements (mg PM per m$^3$ of exhaust) for ULSD and naphtha fuels at B50. EC (shaded) + OC (solid) measurements on the QFF show similar PM collection as the total mass measurements on the TF.

Changes in composition can influence the oxidation behavior of PM, so quartz-fiber filters (QFF) were used to collect PM for TGA analysis during the same B50 runs discussed above. Raw exhaust sampling with a heated filter oven (see Figure 1) enabled the collection of sufficient amounts of PM samples for repetitive measurements.

Because PM was collected on a QFF, the filter weight could not be accurately weighed before the PM collection, and thus the collected PM mass was estimated from the TGA weights according to Equation (1). An assumption that all PM was oxidized or volatilized during the TGA run up to 800°C was made such that the initial TGA filter weight ($m_{Fi}$) minus the final TGA filter weight ($m_{Ff}$) could be used to calculate the total mass of PM loaded on the 2 disk samples studied in each TGA run ($m_{PMt}$); this assumption prevents accounting for ash content in PM samples, which would be counted as part of $m_{Ff}$. Equation (2) indicates point-by-point subtraction of $m_{Ff}$ throughout the TGA, which was applied to the data from each run like a baseline subtraction; e.g., accounting for variations in the bare QFF sample mass from run to run. The resulting $m_{PM(x)}$ data string was subsequently normalized on a point-by-point basis using $m_{PMt}$ as shown in Equation (3) to account for variations in the total PM mass from run to run; the resulting $\%m_{PM(x)}$ distributions showed little deviation between the three TGA runs for each sample. The normalized PM mass loss, $\%m_{PM(x)}$, was averaged from the three runs, and is shown as dashed lines in Figure 5 for both naphtha and ULSD PM samples as a function of oxidation temperature; in this form, the dependent x variable is temperature. Also shown as solid lines in Figure 5, the negative derivative of the PM mass loss as a function of temperature was calculated according to Equation (4). A 10 point moving average was applied to each TGA data set, and the three runs were subsequently averaged for each PM sample. These curves compare the oxidation reactivity of PM samples generated from naphtha and ULSD fuels, and show that naphtha PM is slightly more reactive than ULSD PM.

$$m_{Fi} - m_{Ff} = m_{PMt} \quad (1)$$

$$m_{F(x)} - m_{Ff} = m_{PM(x)} \quad (2)$$

$$\left(m_{PM(x)}/m_{PMt}\right) * 100 = \%m_{PM(x)} \quad (3)$$

$$\left(\%m_{\%PM(x-1)} - \%m_{PM(x)}\right)/(T_x - T_{x-1}) = \delta\left(\%m_{PM(x)}/T_x\right) \quad (4)$$

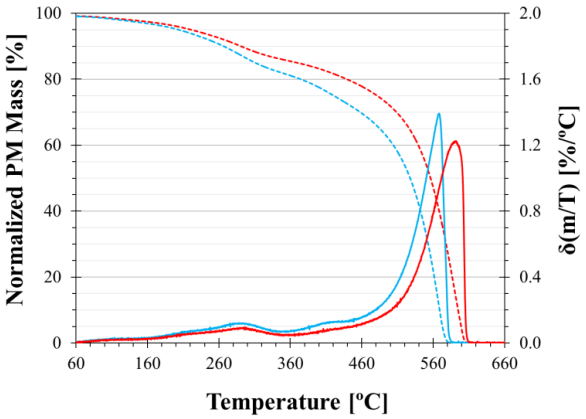


Figure 5. Averaged mass normalized TGA results as a function of temperature. Dashed lines show the normalized mass and the solid lines are the mass derivatives in %/min. The blue plots are PM from Naphtha and red plots are from ULSD.

The TGA gas flow was analyzed by a Mass Spectrometer (MS) downstream of the PM sample, which showed good mass change correlation with $CO_2$ (m/z of 44) production (as shown in Figure 6). Empty TGA–MS temperatures ramps were used as baseline for the reported ionization curves. No $CO_2$ production was measured for the blank filters, thus all $CO_2$ production measured by TGA-MS can be attributed to the oxidation of PM samples. Both fuels show the oxidation peaks near 570ºC, but differ in their main peak oxidation temperature. The low temperature mass changes, which corresponded to $CO_2$ production near 270ºC, can be attributed to a soluble organic faction (SOF) of the soot [11]. The main inflection point of the TGA oxidation data occurs at a slightly lower temperature for the naphtha PM than ULSD, 568ºC and 591ºC, respectively. Despite the difference in specific reactivity between the two PM samples, the shapes of the oxidative reactivity profiles are generally similar for PM from the two fuels. This similar overall oxidation temperature profiles suggest that few changes to the diesel soot oxidation model may be required if using naphtha as a drop-in fuel replacement.

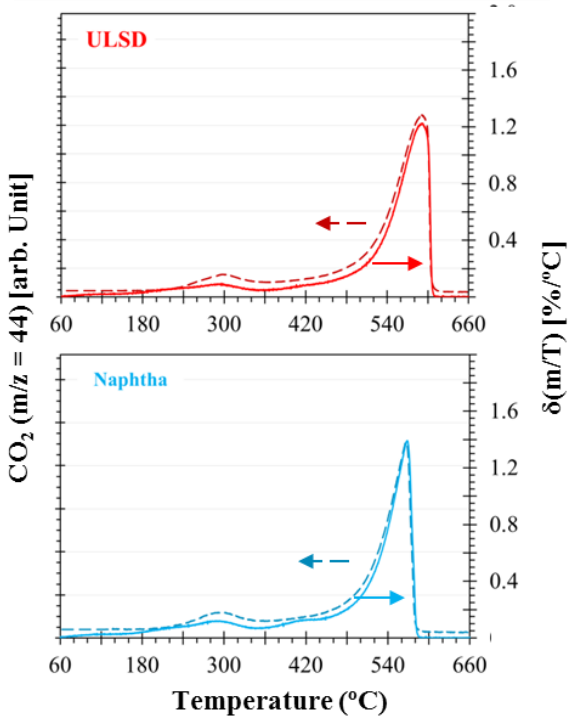


Figure 6. Correlation of PM oxidation with $CO_2$ production from TGA-MS analyses. [dashed line, left y-axis] The $CO_2$ production from TGA TPO ramp based from the mass spectrometer ionization current for m/z =44 as a function of the temperature; [solid line, right y-axis] The negative derivative of the TGA mass loss plot as a function of temperature.

## Summary/Conclusions

In this study, low cetane, low octane naphtha (CN 34, RON 56) was examined as a drop-in fuel on a Cummins ISX15 6-cylinder heavy-duty engine and aftertreatment system without any modifications to the hardware or software calibration.

During the FTP and RMC tests, overall lower $CO_2$ emissions and fuel consumption were measured for naphtha due in part to its higher heating value and higher hydrogen to carbon ratio compared to ULSD. Engine-out and tailpipe NOx were also slightly lower for naphtha fuel. The effects of fuel on engine performance and emissions were further examined at the B50 operating point. Approximately 3% reduction in BSFC was observed, and a significant reduction in PM emissions was achieved with naphtha fuel at an equivalent level of engine-out NOx emissions. A more pronounced premixed combustion was also observed for naphtha fuel, although overall combustion was dominated by mixing-controlled combustion.

Engine-out PM samples were collected at the B50 operating point, and further analyzed to assess the effects of fuel on their chemical composition and oxidation rates. A significant reduction in elemental carbon (EC) in PM samples was observed for naphtha fuel, and is consistent with the corresponding FSN measurements. Similar oxidation rates and peak oxidation temperatures were measured for both fuels, suggesting that similar modeling and control strategies may be used for the two fuels.



## References

1. The Outlook for Energy: A View to 2040, Exxon Mobil, 2016, corporate.exxonmobil.com/en/energy/energy-outlook.
2. U.S. Energy Information Administration, “International Energy Outlook 2014: World Petroleum and Other Liquid Fuels,” 2014.
3. World Energy Council, “World Energy Scenarios” Global Transport Scenarios 2050,” 2011.
4. Zhang, Y., Kumar, P., Traver, M., Cleary, D., “Conventional and Low Temperature Combustion using Naphtha Fuels in a Multi-Cylinder Heavy-Duty Diesel Engine,” SAE Technical Paper 2016-01-0764, 2016, doi:10.4271/2016-01-0764.
5. Akihama, K., Kosaka, H., Hotta, Y., Nishikawa, K., “An Investigation of High Load (Compression Ignition) Operation of the “Naphtha Engine” - a Combustion Strategy for Low Well-to-Wheel CO2 Emissions,” *SAE Int. J. Fuels Lubr.* 1(1):920-932, 2009, doi:10.4271/2008-01-1599.
6. Rose, K., Cracknell, R., Rickeard, D., Ariztegui, J., “Impact of Fuel Properties on Advanced Combustion Performance in a Diesel Bench Engine and Demonstrator Vehicle,” SAE Technical Paper 2010-01-0334, 2010, doi:10.4271/2010-01-0334.
7. NIOSH Manual of Analysis Methods, “Diesel Particulate Matter (as Elemental Carbon),” NIOSH Method 5040, Rev. Mar. 2003.
8. Curran, S., Prikhodko, V., Cho, K., Sluder, S., Parks, J., Wagner, R., “In-Cylinder Fuel Blending of Gasoline/Diesel for Improved Efficiency and Lowest Possible Emissions on a Multi-Cylinder Light-Duty Diesel Engine,” SAE technical paper 2010-01-2206, 2010. doi:10.4271/2010-01-2206
9. Storey, J.E.M., Curran, S.J., Lewis, S.A., Barone, T.L., Dempsey, A.B., Moses-DeBusk, M., Hanson, R.M., Prikhodko, V.Y., Northrop, W.F., “Evolution of Current Understanding of Physicochemical Characterization of Particulate Matter from Reactivity Controlled Compression Ignition Combustion on a Multicylinder Light-Duty Engine,” I*nt. J. Engine Res.* Epub ahead of print 4 August 2016. doi: 10.1177/1468087416661637
10. Reijnders, J., Boot, M., de Goey, P., “Impact of Aromaticity and Cetane Number on the Soot-NOx Trade-Off in Conventional and Low Temperature Combustion,” *Fuel*, 186:24-34, 2016, doi:10.1016/j.fuel.2016.08.009
11. Yezerets, A., Currier, N., Eadler, H., Suresh, A., Madden, P., Branigin, M., “Investigation of the Oxidation Behavior of Diesel Particulate Matter,” Catal. Today, 88: 17-25, 2003, doi:10.1016/j.cattod.2003.08.003

## Contact Information

Jong Lee
Aramco Research Center – Detroit
46535 Peary Court
Novi, MI 48377 USA
jong.lee@aramcoservices.com

## Acknowledgments

The authors gratefully acknowledge all the technical support provided by Lyle Kocher, Sriram Popuri, Suk-Min Moon, Michael Haas and members of the Advanced Engineering Systems Integration team from Cummins Inc. The authors also appreciate the input from engineers, researchers, and technicians at the Aramco Research

Center –Detroit for their contributions to this project and would like to especially thank: Steven Sommers, Michael Zimmermann (ARC), and Todd Carpenter (AVL). Some of the particulate matter data and analysis was conducted at the National Transportation Research Center, a DOE user facility at Oak Ridge National Laboratory.

## Definitions/Abbreviations

| | |
|---|---|
| **ATDC** | After Top Dead Center |
| **ASC** | Ammonia Slip Catalyst |
| **BSFC** | Brake Specific Fuel Consumption |
| **BTE** | Brake Thermal Efficiency |
| **CA** | Crank Angle |
| **CAC** | Charge Air Cooler |
| **CAD** | Crank Angle Degree |
| **CN** | Cetane Number |
| **CO** | Carbon Monoxide |
| **CR** | Compression Ratio |
| **DOC** | Diesel Oxidation Catalyst |
| **DEF** | Diesel Exhaust Fluid |
| **DPF** | Diesel Particulate Filter |
| **EC** | Elemental Carbon |
| **EGR** | Exhaust Gas Recirculation |
| **EO** | Engine-Out |
| **EPA** | Environmental Protection Agency |
| **FIA** | Fluorescent Indicator Adsorption |
| **FSN** | Filter Smoke Number |
| **FTP** | Federal Test Procedure |
| **HC** | Hydrocarbon |
| **HRR** | Heat Release Rate |
| **ID** | Ignition Delay |
| **IMEP** | Indicated Mean Effective Pressure |
| **MY** | Model Year |
| **NIOSH** | Nat'l Inst. for Occupational Safety & Health |
| **NO** | Nitric Oxide |
| **NOx** | Nitrogen Oxides |
| **OC** | Organic Carbon |
| **PM** | Particulate Matter |
| **PPCI** | Partially Premixed Compression Ignition |
| **QFF** | Quartz-Fiber Filter |
| **RMC** | Ramped Mode Cycle |
| **RON** | Research Octane Number |
| **SCR** | Selective Catalytic Reduction |
| **SOF** | Soluble Organic Fraction |
| **SD** | Standard Deviation |
| **TF** | Teflon filter |
| **TP** | Tailpipe |
| **ULSD** | Ultra-Low-Sulfur Diesel fuel |
| **VGT** | Variable Geometry Turbocharger |

# Appendix

All the test results reported in this paper were averaged from at least 3 test results (except cold FTP), and the percent standard deviation (SD) of some of the key measurements are listed in the table A-1.

Table A-1. Engine-out emissions, fuel consumption, and work during the tests

| EO Emissions | | $CO_2$ | | CO | | THC | | NOx | | FC | | Work | |
|---|---|---|---|---|---|---|---|---|---|---|---|---|---|
| | | g/kWh | %SD | g/kWh | %SD | g/kWh | %SD | g/kWh | %SD | g/kWh | %SD | kW | %SD |
| ULSD | cFTP | 774 | N/A | 0.81 | N/A | 0.84 | N/A | 4.23 | N/A | 244 | N/A | 23.2 | N/A |
| | hFTP | 725 | 0.4 | 0.70 | 4.3 | 0.75 | 40.4 | 4.93 | 1.0 | 228 | 0.5 | 23.3 | 0.0 |
| | RMC | 612 | 0.1 | 0.31 | 2.9 | 0.11 | 9.7 | 4.88 | 1.3 | 192 | 0.1 | 118.0 | 0.0 |
| Naphtha | cFTP | 711 | N/A | 1.61 | N/A | 0.95 | N/A | 4.37 | N/A | 230 | N/A | 23.4 | N/A |
| | hFTP | 683 | 1.5 | 1.48 | 9.8 | 0.57 | 40.4 | 4.21 | 6.5 | 221 | 1.7 | 23.4 | 0.0 |
| | RMC | 588 | 0.4 | 0.48 | 8.8 | 0.12 | 19.7 | 4.34 | 5.1 | 189 | 0.4 | 118.3 | 0.2 |